10th International Kimberlite Conference, Bangalore - 2012

10IKC-163

KIMBERLITE ASCENT: CHRONICLES OF OLIVINE

Brett*RC[1], Russell JK[2], and Andrews G[3]

[1]Rio Tinto Exploration Canada Inc. Vancouver, Canada (curtis.brett@riotinto.com)
[2]The University of British Columbia, Vancouver, Canada
[3]University of California Santa Barbara, Santa Barbara California, USA

INTRODUCTION

The ascent and eruption of kimberlite produces volcanic deposits that are anomalously enriched in macrocrysts. The macrocryst population derives mainly from the disaggregation of mantle-derived xenoliths of garnet peridotite. The xenoliths are fragments of mantle wall rock incorporated and buoyed to Earth's surface by kimberlitic magmas over large distances (> 250 km). Many textural and chemical features preserved within these xenocrysts result from physical and chemical changes (P-T-X) during kimberlite ascent and these features can be used to elucidate the transport properties of kimberlite magma.

Olivine is the most abundant mineral in the macrocryst suite and is a good candidate for a textural and chemical study because: (1) it is sensitive and responsive to chemical changes in the kimberlite melt (e.g. SiO_2 content); (2) it is abundant in all kimberlite deposits, and (3) it accompanies magma ascent from source to deposit. Previous studies have utilized mantle-derived olivine to estimate the composition of the mantle (e.g. Griffin et al., 2003) and to calculate stress-states in the mantle (Kennedy et al., 2002). Here we use the textural and chemical properties of kimberlitic olivine to reconstruct the ascent of kimberlite. Kimberlitic olivine phenocrysts host a variety of primary inclusions. For example, mineral inclusions which, used in conjunction with the composition of the host crystal, constrain olivine saturation temperatures (Fedortchouk and Canil, 2004). Melt inclusions are also abundant and provide data on melt compositions, liquidus temperatures and olivine growth (Roedder, 1965; Sobolev et al., 1989). Lastly, fluid inclusions record information on the volatile content of the melt (Kamenetsky et al., 2009). Each of these inclusions on its own contributes to our understanding of kimberlite petrogenesis, however, collectively the nature and relative timing of formation of these features tightly constrains the dynamics of kimberlite ascent.

We present a chronological, textural, and chemical description of kimberlitic olivine and propose a summary kimberlite ascent model. Our textural study is based on intrusive and pyroclastic kimberlite from the Diavik kimberlite cluster, Canada (c.f. Brett et al., 2009), and from the Igwisi Hills kimberlitic lava flows, Tanzania (c.f. Dawson, 1994). These deposits are relatively young (Cenozoic) and their preservation is excellent. These deposits represent different volcanic facies, locations, and eruption times, but show strikingly similar textures. Crosscutting relationships between many of these textures are observed; based on these relationships, and the known intrinsic properties of olivine, we calculate extrinsic properties of the kimberlitic system to provide a basis for our model of kimberlite ascent.

TEXTURAL DESCRIPTION

Olivine xenocrysts are abundant (40 to 50 modal %) and range in diameter from < 0.01 mm - 5 cm. Aspect ratios vary between 1:1 and 2:1. Olivine consists of two types based on shape and size: (1) medium to coarse-grained, rounded to sub-rounded grains, and (2) fine-grained (< 1 mm), euhedral to subhedral crystals. All olivine have thin overgrowths (<150 microns) which are chemically distinct with respect to the cores (c.f. Brett et al., 2009). Large cores have euhedral overgrowths (Fig. 1a) and small cores have anhedral overgrowths (Fig. 1b). The cores are well rounded (Fig. 1c-e) and are intensely fractured by sub-parallel networks of micro-cracks at approximately orthogonal angles (Fig. 1f-i). The fractures terminate on the outside surface against the overgrowths of olivine implying that the overgrowths post-date the internal fracturing (Fig. 1a-b, f-h) and contain fluid, mineral and crystallized melt as inclusions (Fig. 1a-b, h).

Two types of fracture sets occur in the cores of olivine: (1) tens of sub-parallel, planar cracks of varying aperture (<5 μm) that are sealed by carbonate and are referred to as "sealed cracks" (Fig. 1f-g); and (2) numerous planar to curvilinear cracks having all of the features characteristic of crack-healing processes (c.f. Smith and Evans, 1984; Fig. 1 h-k). In cross-section, the carbonate infill in the sealed cracks (Fig. 1f-g) is defined by a linear trend marked by patches of elongate carbonate crystals, and can contain other solid phases (e.g., Mg-chromite; Fig. 1g) and terminate at the core-overgrowth interface (Fig. 1f).

The second type of crack is present as partially to fully

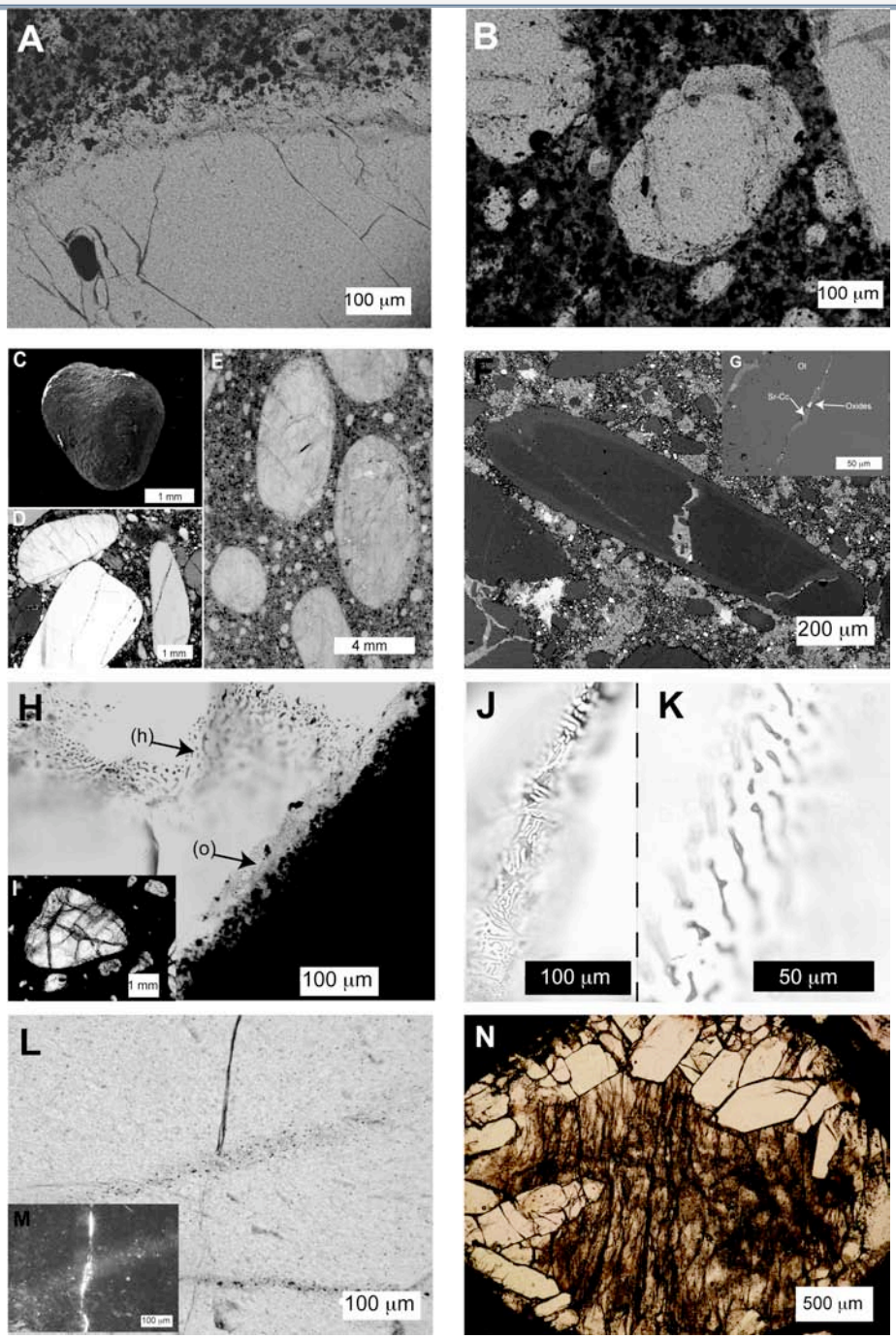

Figure 1. Photomicrographs showing textural features and crosscutting relationships in kimberlitic olivine. (A) Overgrowth on larger (> 1 mm), olivine xenocrysts are too thin to modify overall shape of original rounded olivine grains; (B) Overgrowths on smaller (~200 mm), rounded olivine xenocrysts within kimberlite creating euhedral, phenocryst-like, olivine grains; (C) BSE image of an olivine grain picked from coherent kimberlite (Diavik) and showing the well-rounded, sub-spherical geometry common to most kimberlitic olivine. Photomicrographs of kimberlite showing extreme rounding of olivine xenocrysts in samples from: (D) Diavik and (E) Igwisi Hills; (F) back-scattered electron (BSE) image of sealed cracks contained within a xenocrystic core of olivine (darker grey; Diavik sample) and bounded by an overgrowth of lower forsterite olivine (lighter grey), the inset, (G) shows (BSE) image of a sealed crack within an olivine xenocryst (Diavik), filled by Sr-rich calcite (Sr-Cc) and oxides (Mg-chromite); (H) Healed crack (h) within an olivine from Diavik defined by the distribution of residual inclusions and terminated against the olivine overgrowth (o). The inclusions within the healed cracks are much more abundant and have a very different morphology compared to the inclusions in the overgrowth, the inset (I) shows networks of healed fractures (dark bands) in a single xenocryst; (J) interconnected dendritic networks of inclusions; (K) long irregular vermicular inclusions; (L) Photomicrograph (ppl) of olivine (Diavik) showing a sealed crack that is overprinted by a later healed crack, the inset (M) is the same image as (L) under xpl highlighting the carbonate-filled sealed crack (bright white) in the olivine at extinction (black) that has been overprinted by a healed crack; (N) micrograph of olivine neoblasts showing overprinting networks of healed and sealed cracks (ppl; Igwisi Hills).

healed cracks which show typical healed crack network morphologies (Fig.1h-k) occurring as sub-parallel networks, which are much more numerous than the sealed crack networks (Fig. 1i). The healed cracks (Fig. 1h-k) are present in virtually all olivine crystals and, like the sealed cracks, the healed cracks terminate at the core-overgrowth interface (Fig. 1h). A spectrum of inclusion morphology ranges from connected tubules (partially healed; Fig. 1j) and isolated tubules (Fig. 1k) to fully healed, where they are present as rounded inclusions. Inclusions are brownish and fluidal-like with no discernable crystalline habits and are typically < 5 µm in diameter and contain transparent centers with dark brown rims. The elongate tubules have a maximum width of 5 µm and can be 10 times as long. The healed cracks overprint the sealed cracks (Fig. 1l-m) marking two different generations of cracks that are filled with intrinsically different material; an early 'fill' material that crystallizes as carbonate and a later, potentially more hydrous, fill material that facilitates annealing of the host olivine crystal.

Fine- to coarse-sized tabular crystals (neoblasts) set in strained xenocrystic olivine are common (Fig. 1n; c.f. Arndt et al., 2010) in both Igwisi Hills and Diavik rocks. The neoblasts are strain free (perfect extinction in cross-Nichols), contain no inclusions, and are not cracked. Figure 1n clearly shows that these crystals overprint most of the textures described above. As all of these textural events occur after xenolith incorporation but before emplacement, it is implicit that all features are formed during the ascent of kimberlite. Below we will discuss the physical and chemical processes responsible for the generation of the textures shown in olivine, and use the physical properties of olivine to calculate extrinsic properties of the ascending system.

DECOMPRESSION CRACKING

Olivine crystals transported upward in a lithostatic column are subject to a decrease in lithostatic pressure. Minerals respond to decompression by increasing in volume (Le Chatelier's principle) and can achieve this viscously by changes in either bond angles and/or bond lengths (Lange, 2007). If decompression occurs at a faster rate than the mineral bonding can relax (defined by its Newtonian viscosity) to allow expansion then internal stresses accumulate. If internal stresses exceed the tensile strength of olivine (500 MPa; Johnson and Jenkins, 1991; Roedder, 1984) the crystal will fail in tension (i.e. it will crack).

We modeled the stress state of OH-saturated olivine in an ascending fluid at lithostatic pressures (250 km to surface), at 1300ºC, to predict the amount of decompression required to cause cracking of olivine crystals. The total amount of expansion acting to dissipate the stress caused by ascent is a function of the bulk modulus of olivine (K_T=1.4E11 Pa; Zha et al., 1996), the pressure difference caused by ascent (i.e. $\rho g[z - z_0]$), the ascent velocity (V) and the Newtonian viscosity of wet olivine ($\eta=10^{17}$ Pa; Karato and Jung, 2003). The stress state of an olivine crystal is modeled for two ascent velocities (20 m/s and 0.1 m/s) that bracket current ascent rate estimates for kimberlite (Sparks et al., 2006). Ascent at 20 m/s causes cracking after ~17 km (~14 minutes) and ascent at 0.1 m/s causes cracking after ~19 km (just over 2 days) from the point at which the olivine grains were sampled from the mantle wall rocks.

Polymineralic rocks are generally weaker by a factor of ~10 than the minerals that comprise the rock; coarse-grained rocks are generally weaker than fine-grained rocks because longer grain boundaries provide longer pathways of weakness (Eberhardt et al., 1999). Coarse-grained peridotite xenoliths reach their tensile strength and begin to break apart after a ~50 MPa pressure drop, or approximately after 2 km of ascent whereas fine-grained peridotite requires upward of 7 km of ascent to cause disaggregation.

DISCUSSION OF KIMBERLITE ACSENT

Ultramafic xenoliths, and their disaggregated components are transported by kimberlitic volcanism from mantle depths of > 250 km (e.g. Boyd and Nixon, 1975). The most likely mechanisms for wall-rock fragmentation of peridotite are dyke propagation and emplacement (Johnson and Pollard, 1973; Rubin, 1995) and/or degassing and gas streaming at mantle depths (Lensky et al., 2006; Wyllie, 1980) exacerbated by the low viscosity of alkaline magmas (Sparks et al., 2006) which causes more intense fracturing of the country rocks (Rubin, 1993). Xenoliths are buoyed by low-density fluid and begin to disaggregate after 2-7 km of ascent. Very large xenocrysts have been recorded in kimberlite up to 10 cm in diameter (Schulze, 2001); whereas, there are virtually no xenoliths observed that comprise megacrystic-sized olivine. In fact most xenoliths in kimberlite are made up of smaller grain sizes (< 0.5 mm). This is consistent with our model, which suggests that coarse-grained peridotite will disaggregate rapidly and efficiently during ascent (i.e. depressurization), whereas fine-grained peridotite requires larger pressure drops to generate the same degree of disaggregation.

Decompression causes the olivine crystals to crack after approximately 19 km of upward travel; the space produced by cracking is filled by solid, liquid, and supercritical phases. The first generation of cracks is filled with melt and crystals consisting of primary carbonate (high-Sr), chromite, and spinel crystals. The carbonate fluid later crystallizes and seals fractures. The presence of carbonate and oxides in these cracks is evidence that: (1) oxide phases have crystallized at great depth; and (2) the kimberlite melt/fluid is capable of crystallization of carbonate enriched in Sr and Ba at depth (c.f. Armstrong et al., 2004). The carbonate in the decompression cracks is > 90% $CaCO_3$ and implies that the kimberlite melt is carbonatite like in composition. These observations are in agreement with recent experiments that suggest that all kimberlite melts originate as carbonatitic-melts (c.f. Russell et al., This

Volume). Experiments on $CaCO_3$-$MgCO_3$ solid solutions show that at high pressure (1 GPa) calcite is the only stable carbonate phase if the melt is composed of < 20 mole% of the $MgCO_3$ component (Buob et al., 2006). The carbonate sealant in these fractures thus represents kimberlitic material sampled at a relatively unevolved point in the kimberlitic magmas evolution.

The mechanism responsible for rounding the olivine xenocrysts occurs after disaggregation, but before overgrowth production. The well-rounded megacrystic texture observed in kimberlite dykes and flows is consistent with breccia textures formed by explosion or fluidization at depth (Morin and Corriveau, 1996). Olivine surfaces can feature dissolution textures (e.g. Donaldson, 1976, 1990); however, these textures are not consistent with the polished and rounded textures observed in kimberlite (Fig. 1c-e). It is for this reason that we interpret olivine rounding to be caused by a fluidised suspension of solids and gas. An industrial analogue to this rounding process is a jet mill (Tuunila, 1997), which forces a solid and gas mixture at high flow rates to produce a rounded, narrow particle distribution, very quickly. Fluidisation is turbulent in order to maximize particle-particle collisions required for rounding.

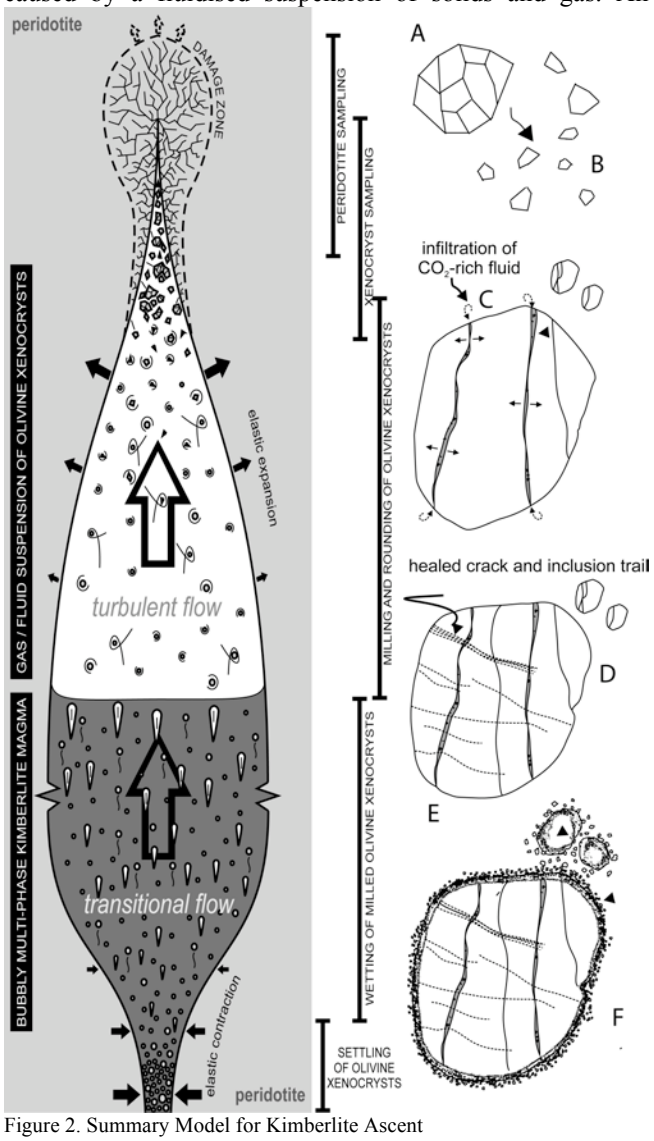

Figure 2. Summary Model for Kimberlite Ascent

Decompression cracking is continuous in xenocrysts, and subsequent cracking overprints previous sealed cracks. Similar to the formation of sealed cracks, healing requires external fluids to in-fill void space created by cracking. Dissolution and crystallization of the host mineral along crack surfaces (i.e. olivine) decreases the surface energy of the crack, and drives the in filled-fluid to form spherical shapes surrounded by the newly crystallized host mineral (i.e. necking down; Roedder, 1984). Kimberlitic fluids are not in equilibrium with orthopyroxene xenocrysts derived from peridotite (Kopylova et al., 2007), and as xenocrysts dissolve the melt becomes more siliceous and drives the system to saturate with olivine (Brett et al., 2009). The healed cracks thus trap and record compositions in this regime. The healing rates of these cracks have been determined to happen in hours to several days (Wanamaker et al., 1990).

The overgrowths observed on rounded olivine crystals enclose sealed cracks and healed cracks and therefore must occur later in time. The environment has to be siliceous and more melt-like than the gaseous, $CaCO_2$-dominated fluid responsible for carbonate in filled sealed cracks. This implies a transition from a multiphase gas/fluid environment to denser, siliceous, bubbly kimberlite magma. Olivine xenocrysts seed olivine growth at saturation and causes growth of olivine rims, which traps phases (solid, liquid and/or gas), preserving them as inter-crystalline inclusions. Effervescence of volatile phases (i.e. CO_2) is facilitated by nucleation on preexisting xenocrystic surfaces. Contemporaneous saturation and growth of olivine traps these bubbles as planes of fluid phases inside the crystal (Fig. 1a-b, h). An important observation is that olivine phenocrysts and overgrowths are not fractured; this implies that the saturation of olivine can only occur less than 19 km from earth's surface (else we would expect cracks).

The crack-free and inclusion-free nature of the neoblasts is sufficient evidence to support that static re-crystallization of strained olivine xenocrysts happens during the ascent of kimberlite. The size of annealed neoblasts has been used to estimate the ascent rate of kimberlite (Mercier, 1979), where larger (1 mm) neoblasts have been estimated to anneal over 4-6 hours and are consistent with the ascent velocity and time scales used in this study.

SUMMARY

Olivine is supplied to kimberlitic melts at depth by the entrainment of peridotitic mantle xenoliths (Fig. 2a) that rapidly disaggregate due to the decompression. During

ascent within the mantle, path lengths of 2-7 km (100 – 350 s at 20 m/s) are suffice to cause pressure drops that cause peridotite to fail in tension. This produces a population of olivine xenocrysts that are released to the fluid filled turbulent dyke-tip (Fig 2b). Continued, rapid and accelerating ascent (due to expansion) supports continued and increasing rates of decompression. Path lengths of ~19 km of ascent (52 hours – 15 minutes at ascent rates of 0.1 to 20 m/s) are suffice to cause individual olivine crystal to fail in tension and form cracks (Fig. 2c). Small wetting-angles between fluid and olivine allow infiltration of carbonate-fluid and oxide phases that seal the cracks. Turbulent flow encourages mechanical rounding or milling of the xenocrysts (Fig. 2d). Dense olivine xenocrysts sink through the column of kimberlite froth into kimberlite magma. As decompression continues, a generation of later cracks overprints the carbonate-filled sealed cracks. This generation of cracks is filled by melt and fluid that promotes healing of these cracks and heals on the time-scales of minutes to hours, trapping inclusions (Fig. 2e). Xenocrysts that sediment through the column act as nucleation sites when the melt subsequently becomes saturated with olivine within 19 km of Earth's surface and all olivine crystals are rimmed with olivine of lesser forsterite component (Fig. 2f). The proposed model is built on crucial petrographic observations and serves as a chronological series of textural events for which an evolution of the chemistry of kimberlite, and extrinsic (P, T) properties of specific volcanic processes can be indirectly assessed.

REFERENCES

Armstrong, J., Wilson, M., Barnett, R., and Nowicki, T., 2004, Mineralogy of primary carbonate-bearing hypabyssal kimberlite, Lac de Gras, Slave Province, …: Lithos.

Arndt, N. T., Guitreau, M., Boullier, A.-M., Le Roex, A., Tommasi, A., Cordier, P., and Sobolev, A., 2010, Olivine, and the Origin of Kimberlite: Journal of Petrology, v. 51, no. 3, p. 573-602.

Boyd, F. R., and Nixon, P. H., 1975, Origins of ultramafic nodules from some kimberlites of Northern Lesotho and the Monastery Mine, South Africa.: Phys. Chem. Earth, v. 9, p. 431-454.

Brett, R. C., Russell, J. K., and Moss, S., 2009, Origin of olivine in kimberlite: Phenocryst or impostor?: Lithos, v. 112, p. 201-212.

Buob, A., Luth, R., Schmidt, M., and Ulmer, P., 2006, Experiments on CaCO3-MgCO3 solid solutions at high pressure and temperature: American Mineralogist.

Dawson, J., 1994, Quaternary kimberlitic volcanism on the Tanzania Craton: Contributions to Mineralogy and Petrology.

Donaldson, C., 1976, An experimental investigation of olivine morphology: Contributions to Mineralogy and Petrology.

-, 1990, Forsterite dissolution in superheated basaltic, andesitic and rhyolitic melts: Mineralogical Magazine.

Eberhardt, E., Stimpson, B., and Stead, D., 1999, Effects of grain size on the initiation and propagation thresholds of stress-induced brittle fractures. : Rock Mechanics and Rock Engineering, v. 32, no. 2, p. 81-99.

Fedortchouk, Y., and Canil, D., 2004, Intensive Variables in Kimberlite Magmas, Lac de Gras, Canada and Implications for Diamond Survival: Journal of Petrology, v. 45, no. 9, p. 1725-1745.

Griffin, W., O'Reilly, S., Abe, N., and Aulbach, S., 2003, The origin and evolution of Archean lithospheric mantle: Precambrian Research.

Johnson, A. M., and Pollard, D. D., 1973, Mechanics of growth of some laccolithic intrusions in the Henry Mountains, Utah, I: Field observations, Gilbert's model, physical properties and flow of the magma.: Tectonophysics, v. 18, p. 261-309.

Johnson, E., and Jenkins, D., 1991, Synthetic H 2 O---CO 2 fluid inclusions in spontaneously nucleated forsterite, enstatite, and …: Geochimica et Cosmochimica Acta.

Kamenetsky, V. S., Maas, R., Kamenetsky, M. B., Paton, C., Phillips, D., Golovin, A. V., and Gornova, M. A., 2009, Chlorine from the mantle: Magmatic halides in the Udachnaya-East kimberlite, Siberia: Earth and Planetary Science Letters, v. 285, no. 1-2, p. 96-104.

Karato, S., and Jung, H., 2003, Effects of pressure on high-temperature dislocation creep in olivine: Philosophical Magazine.

Kennedy, L., Russell, J., and Kopylova, M., 2002, Mantle shear zones revisited: The connection between the cratons and mantle dynamics: Geology.

Kopylova, M. G., Matveev, S., and Raudsepp, M., 2007, Searching for parental kimberlite melt: Geochimica et Cosmochimica Acta, v. 71, p. 3616-3629.

Lange, R., 2007, The density and compressibility of KAlSi3O8 liquid to 6.5 GPa: American Mineralogist.

Lensky, N., Niebo, R., Holloway, J., Lyakhovsky, V., and Navon, O., 2006, Bubble nucleation as a trigger for xenolith entrapment in mantle melts: Earth and Planetary Science Letters, v. 245, no. 1-2, p. 278-288.

Mercier, J. C. C., 1979, Peridotite xenoliths and the dynamics of kimberlite intrusion: F.R. Boyd and H.A.O. Meyer, Editors, The Mantle Sample, American Geophysical Union, Washington, DC p. 1971.

Morin, D., and Corriveau, L., 1996, Fragmentation processes and xenolith transport in a Proterozoic minette dyke, Grenville Province, Quebec: Contrib Mineral Petrol, v. 125, p. 319-331.

Roedder, E., 1965, Liquid CO2 inclusions in olivine-bearing nodules and phenocrysts form basalts: The American Mineralogist, v. 50, p. 1746-1782.

Roedder, E., 1984, Fluid inclusions : an introduction to studies of all types of fluid inclusions, gas, liquid, or melt, trapped in materials from earth and space, and their appplication to the understanding of geologic processes, [Washington,D.C.], Mineralogical Society of America, Reviews in mineralogy,, v. 12, vi, 644 p. p.:

Rubin, A., 1995, Propagation of magma-filled cracks: Annual Review of Earth and Planetary Sciences.

Rubin, A. M., 1993, Tensile fracture of rock at high confiining pressure: implications for dike propagation: Journal of Geophysical Research, v. 98, no. 15, p. 919-935.

Schulze, D. J., 2001, Origins of chromian and aluminous spinel macrocrysts from kimberlites in Southern Africa: The Canadian Mineralogist, v. 39, p. 361-376.

Smith, D., and Evans, B., 1984, Diffusional crack healing in quartz: Journal of Geophysical Research.

Sobolev, A. V., Sobolev, N. V., Smith, C. B., and Dubessy, J., 1989, Fluid and melt compositions in lamproites and kimberlites based on the study of inclusions in olivine: GAS Special Publication No. 14: Kimberlites and related rocks, their composition, occurrence origin and emplacement, v. 1.

Sparks, R., Baker, L., Brown, R., and Field, M., 2006, Dynamical constraints on kimberlite volcanism: J Volcanol Geoth Res.

Tuunila, R., 1997, Ultrafine grinding of FGD and phosphogypsum with an attrition bead mill and a jet mill: Ph.D. Thesis, Lappeenranta University of Technology.

Wanamaker, B., Wong, T., and Evans, B., 1990, Decrepitation and crack healing of fluid inclusions in San Carlos olivine: Journal of Geophysical Research, v. 95, no. B10.

Wyllie, P. J., 1980, The origin of kimberlites: Journal of Geophysical Research, v. 85, p. 6902-6910.

Zha, C., Duffy, T., Downs, R., Mao, H., and Hemley, R., 1996, Sound velocity and elasticity of single-crystal forsterite to 16 GPa: Journal of Geophysical Research.